

# Thermal-Conductivity Measurements of Polymers by a Modified $3\omega$ Technique

Ming Gu · Jian-li Wang · Xing Zhang

Received: 14 March 2009 / Accepted: 15 June 2009 / Published online: 30 June 2009  
© Springer Science+Business Media, LLC 2009

**Abstract** A modified  $3\omega$  technique is designed for measurement of the thermal conductivity of polymers. In this study, samples are prepared by pressing a platinum (Pt) hot wire into melt polymers, and a LabVIEW-based virtual lock-in amplifier is employed to collect the third harmonic of the voltage across the hot wire, which has proved to overcome the disadvantages of the commercial lock-in amplifier, such as inaccuracy at low frequency, lack of flexibility/scalability, and high cost. Three kinds of commercial polymers are measured at room temperature, and the results are checked against data from the literature, which demonstrates that the modified technique can be used with high accuracy and good reproducibility.

**Keywords** LabVIEW · Polymers · Thermal conductivity ·  $3\omega$  method · Virtual lock-in-amplifier

## 1 Introduction

In recent years, there has been an increasing need for reliable thermal conductivity data of polymers, which can not only give theoretical support to an understanding of structure/property relationships of polymers, but also help to improve product quality in polymer processing. Although a number of correlations [1,2] associating such structural variables as molar mass, crystallinity, orientation, etc. with the thermal conductivity have been proposed, the development of effective, accurate measurement

---

M. Gu · J. Wang · X. Zhang (✉)  
Key Laboratory for Thermal Science and Power Engineering of Ministry of Education,  
Department of Engineering Mechanics, Tsinghua University, Beijing 100084, China  
e-mail: x-zhang@tsinghua.edu.cn

M. Gu  
e-mail: gum07@mails.tsinghua.edu.cn

techniques is still necessary and essential. Since Cahill [3] first applied the  $3\omega$  method to measure the thermal conductivity of dielectric solids over a large range of temperature, many  $3\omega$  systems have been constructed for different measurement situations and purposes [4,5]. The most attractive advantage of the method is its capacity for measuring the thermal conductivity and thermal diffusivity simultaneously and for effectively eliminating the radiation effect. However, most of the reported systems utilized commercial lock-in amplifiers to track the  $3\omega$  signals, which have some disadvantages such as (i) poor performance at low frequency for most of them; (ii) lack of flexibility and scalability, such as dynamic reservation limit and one single signal processing unit for one apparatus; and (iii) high cost. Those problems could be unavoidable when the frequency of interest is below 1 Hz or two or more signals need to be analyzed at one time.

In this article, a modified  $3\omega$  measurement technique is developed to measure the thermal conductivity of polymers. Counter to common practice for  $3\omega$  measurements, the sample is prepared by pressing an ac excited hot wire into the interface of two polymers in the molten state, and, a LabVIEW-based virtual lock-in amplifier is employed to detect the faint signals. This  $3\omega$  technique has proved to be an effective way to determine the thermal conductivity of polymers while repressing those drawbacks mentioned above. Through measuring different kinds of commercial polymers at room temperature and comparing the results with the literature, the reliability of the method has been demonstrated.

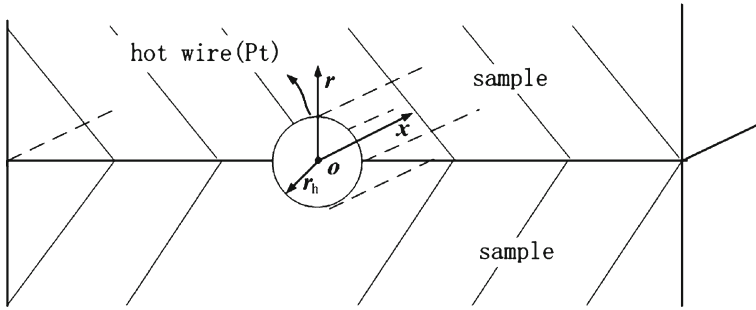
## 2 Principle of Measurement

Figure 1 shows a side view of the hot wire and sample geometry. A hot wire of length  $l_h$  and radius  $r_h$  is inserted into the polymer interface. An alternating current (ac) of the angular frequency  $\omega$  flows through the wire and generates heat at an angular frequency  $2\omega$ . This heat induces a temperature fluctuation with the same frequency. It is assumed that the wire is thermally short in the radial direction so that the temperature is uniform over its cross section. Since the electrical resistance of the wire is modulated by the average temperature rise, the voltage across the wire contains a third harmonic component with angular frequency  $3\omega$ . This component contains the information about the thermal properties (thermal conductivity, thermal diffusivity) of tested polymers surrounding the hot wire, and by measuring the frequency dependence of the  $3\omega$  voltage, these thermal properties can be finally determined.

In the case of axis symmetry and  $l_h \gg r_h$ , the model can be treated as a one-dimensional quasi-steady heat conduction model. Due to infinite solid approximation, when an ac  $I_0 \sin(\omega t + \phi_0)$  is applied, the model is given as

$$\frac{1}{\alpha_s} \frac{\partial T_s(r, t)}{\partial t} = \frac{\partial^2 T_s(r, t)}{\partial r^2} + \frac{1}{r} \frac{\partial T_s(r, t)}{\partial r} \quad r \geq r_h \quad (1)$$

$$\frac{1}{\alpha_h} \frac{\partial T_h(t)}{\partial t} = \frac{p - p'}{l_h \pi r_h^2 \lambda_h} \quad r \leq r_h \quad (2)$$



**Fig. 1** Side view of the hot wire and sample geometry. A metal line is placed on the interface of the two semi-infinite samples

where  $\alpha$  is the thermal diffusivity, defined by  $\alpha = \lambda/(\rho c_p)$ ,  $R$  is the electrical resistance of the hot wire, and  $\lambda, \rho, c_p, l$ , and  $r$  are the thermal conductivity, the density, the specific heat, the length, and the radius, respectively. The index  $s$  denotes the sample, and  $h$  denotes the hot wire. The parameters  $p$  and  $p'$ , which are caused by Joule heating and heat transfer from the hot wire to the sample accordingly, are expressed by

$$p = I_0^2 \sin^2(\omega t + \varphi_0) R \tag{3}$$

$$p' = -2\pi r_h l_h \lambda_s \left. \frac{\partial T_s(r, t)}{\partial r} \right|_{r_h} \tag{4}$$

The average volumetric temperature rise of the hot wire  $\Delta T_h$  is obtained analytically as

$$\Delta T_h(t) = \Delta T_{dc} + \text{Re} [\bar{u} \exp [2(\omega t + \varphi_0)i]] \tag{5}$$

where  $\Delta T_{dc}$  is a temperature rise independent of frequency, and the form of  $\bar{u}$  is

$$\bar{u} = -\frac{I_0^2 R}{4\pi l_h \lambda_s k r_h i^{1/2}} \frac{K_0(k r_h i^{1/2})}{K_1(k r_h i^{1/2}) + (\rho C_p)_h r_h^2 i \omega K_0(k r_h i^{1/2})} \tag{6}$$

Here,  $K_0$  and  $K_1$  are the zero- and first-order modified Bessel functions, and  $k^{-1}$  is the thermal penetration depth, defined by  $k^{-1} = (2\omega/\alpha_s)^{-1/2}$ .

According to the  $R - T$  correlation of the hot wire, the overall voltage across it, consisting of two  $1\omega$  components and one  $3\omega$  component, can be obtained:

$$\begin{aligned} V_h(t) &= I_0 \sin(\omega t + \varphi_0)(R + R' \Delta T_h) \\ &= I_0 \sin(\omega t + \varphi_0)(R + R' \Delta T_{dc}) - u_{3\omega} \sin(\omega t + \varphi_0 + \theta_{3\omega}) \\ &\quad + u_{3\omega} \sin(3(\omega t + \varphi_0) + \theta_{3\omega}) \end{aligned} \tag{7}$$

where the amplitude  $u_{3\omega}$  and the phase  $\theta_{3\omega}$  of the  $3\omega$  component are expressed by

$$u_{3\omega} = \frac{I_0 R'}{2} \sqrt{\text{Re}(\bar{u})^2 + \text{Im}(\bar{u})^2} \quad (8)$$

$$\theta_{3\omega} = \arctan [\text{Im}(\bar{u})/\text{Re}(\bar{u})] \quad (9)$$

where  $R'$  is a coefficient proportional to the temperature coefficient of the resistance (TCR) of the hot wire, and Re and Im represent the real part and imaginary part of plurality. In this study, the thermal conductivity of polymers is determined by curve-fitting the analytical model of Eq. 8 to experimental data using a least-squares approach.

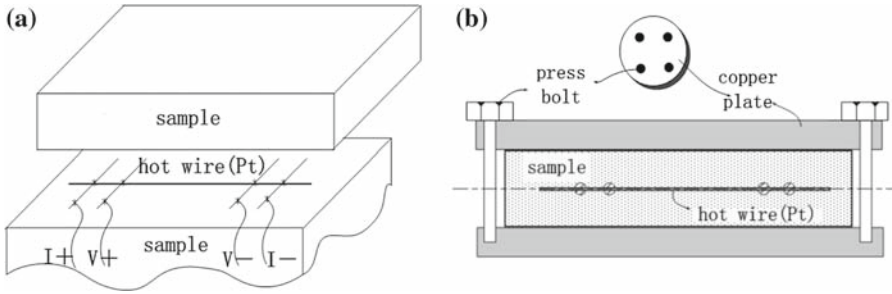
### 3 Experiments

#### 3.1 Sample Preparation

For the measurements, polymer samples are prepared in the shape of rectangles with thicknesses of 2 mm to 3 mm. The infinite solid approximation could be satisfied by carefully selecting the frequency to make the thermal penetration depth much less than the thicknesses of samples. For this study, the thermal penetration depth is from 0.2 mm to 0.02 mm at frequencies from 0.1 Hz to 10 Hz, meeting the infinite solid assumption. A platinum wire (purity, 99.98%; length, 10 mm; diameter, 30  $\mu\text{m}$ ) is chosen as a hot-wire probe. As shown in Fig. 2a, the hot wire is welded to four copper wires (diameter, 100  $\mu\text{m}$ ) to form a four-wire configuration. The configuration is then placed at the middle of two tested polymers. Figure 2b shows a schematic diagram of the equipment to press the two polymers together. First, the two-folded polymers with the probe at the middle of them are placed between two copper plates. Then the entire sandwich-like configuration is put into a furnace to be heated to the melting point of the polymers for several minutes until the two-folded polymers reach the molten state. Once the molten state is achieved, the four bolts are fastened and adjusted to produce a pressure. Then, the hot wire can be pressed into the samples and to maintain tight contact with the polymers because of the pressure. After the pressing process, the sample is cooled to room temperature before the measurement.

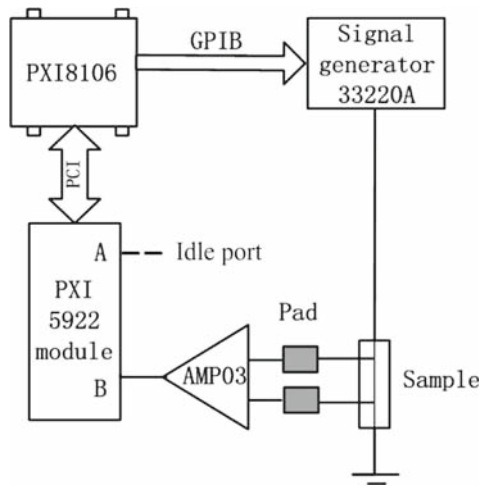
#### 3.2 Measurement System

Figure 3 shows the circuit diagram of the  $3\omega$  measurement system. The system is similar to that of Cahill, except there is no need of subtracting the  $1\omega$  voltage in the circuit and a LabVIEW-based virtual lock-in-amplifier is designed to replace the commercial instrument as the detector of  $3\omega$  signals. Here, a function generator (Agilent 33220A) with an internal resistance of 50  $\Omega$  is controlled by an industrial computer (PXI 8106) through GPIB to produce sine waves of a series of frequencies. A two-channel 24-bit high-speed analog-to-digital converter (ADC) (PXI 5922) is used to convert the analog voltage signals exported by differential amplifiers (AMP03) to digital



**Fig. 2** Schematic diagram of preparing the sample and the probe: **(a)** perspective view and **(b)** side view

**Fig. 3** Schematic diagram of the electrical circuit



signals. Then, the digital signals are transferred to the industrial computer by PCI to be processed. In the computer, the  $3\omega$  signals are finally extracted from the data of five wave periods sampled at a rate of 50,000 Hz.

In this system, the virtual lock-in technique is the most advantageous feature, which is carried out through three main steps in the LabVIEW program: (a) a pair of reference signals  $\sin(3\omega t)$  and  $\cos(3\omega t)$  are simulated by the program and then multiplied by the voltage across the hot wire (Eq. 7) to produce two signals consisting of dc and ac components; (b) after the ac components are suppressed by a first-order, low-pass filter, two dc signals can be obtained, which are  $e_1 = 0.5u_{3\omega} \cos(3\phi_0 + \theta_{3\omega})$  and  $e_2 = 0.5u_{3\omega} \sin(3\phi_0 + \theta_{3\omega})$ ; and (c) then, the phase and the amplitude of the  $3\omega$  voltage can be calculated from the forms of  $\theta_{3\omega} = \arctan(e_2/e_1) - 3\phi_0$  and  $u_{3\omega} = (2e_1 + 2e_2)/\{\cos[\arctan(e_2/e_1)] + \sin[\arctan(e_2/e_1)]\}$ , respectively.

Comparing with traditional  $3\omega$  measurement systems, this  $3\omega$  system is highly improved in three aspects. First, because there is no dynamic reservation limit in the virtual lock-in amplifier, it is not necessary to eliminate the  $1\omega$  voltage by using additional circuits like series resistors or balanced bridges. Attributed to that, the system

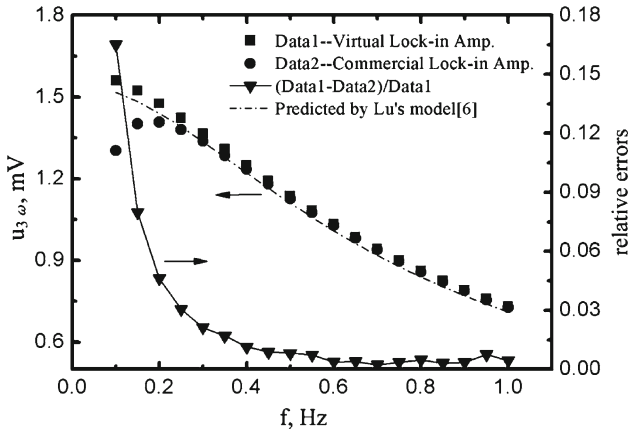


**Fig. 4** Comparison of the amplitude of the  $3\omega$  voltage measured by the two systems. *Solid squares* represent the data of the virtual lock-in amplifier, *solid circles* represent the data of the commercial lock-in amplifier, *triangles* represent the relative errors, and *dashed lines* represent the predicted result

can be largely simplified and, at the same time, the noises caused by these accessory electronic devices can be avoided. Secondly, since the analog-to-digital converter has two channels, two different signals can be processed synchronously if needed. Furthermore, a more user-friendly virtual front panel is designed in the LabVIEW program, from which parameters can be set and results can be displayed directly.

#### 4 Results and Discussion

To evaluate the capability of our virtual lock-in amplifier, a Pt wire (purity, 99.98%; diameter,  $10\ \mu\text{m}$ ; density,  $21460\ \text{kg}\cdot\text{m}^{-3}$ ) with known thermal properties ( $\lambda$ ,  $71.6\ \text{W}\cdot\text{m}^{-1}\cdot\text{K}^{-1}$ ;  $c_p$ ,  $133\ \text{J}\cdot\text{kg}^{-1}\cdot\text{K}^{-1}$ ), is placed in a vacuum chamber at room temperature and measured by the system with the virtual lock-in amplifier and the system with a commercial instrument (7265 DSP) separately. Figure 4 shows a comparison between the amplitude of the  $3\omega$  voltage measured by the two systems. It is obvious that the data from the commercial lock-in amplifier mismatch the results predicted by Lu's model [6] at a frequency lower than 0.4 Hz, while the virtual one performs well over the whole frequency range from 0.1 Hz to 1 Hz. It is illustrated in Fig. 4 that the difference between them decreases sharply with increasing frequency, and is less than 1% at a frequency higher than 0.4 Hz. The same phenomenon can also be found in the measured results of the phase of the  $3\omega$  voltage (Fig. 5). The results demonstrate that the virtual instrument works extremely well as a substitute for the commercial one, with higher accuracy at very low frequencies.

In this study, the  $1\omega$  voltage across a variable resistance box (ZX74B) is employed as an external reference signal and applied to the REF IN connector on the front panel of the 7265 DSP. This setting produces an uncertainty of 0.001 Hz to lock-in frequencies, which cause different degrees of deviations of the measured amplitudes from the target ones (the star shape in Fig. 6) at different frequencies. As shown in

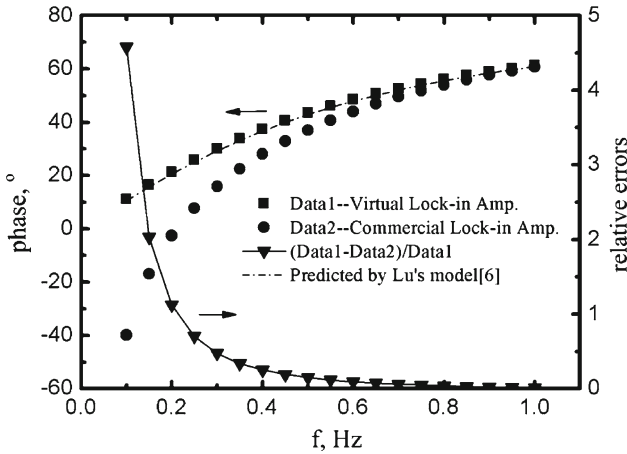


**Fig. 5** Comparison of the phase of the  $3\omega$  voltage measured by the two systems. *Solid squares* represent the data of the virtual lock-in amplifier, *solid circles* represent the data of the commercial lock-in amplifier, *triangles* represent the relative errors, and *dashed lines* represent the predicted result

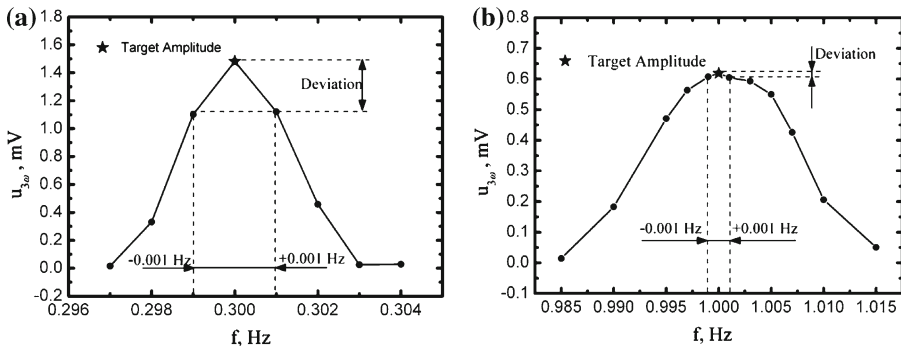


**Fig. 6** The error of the amplitude of the  $3\omega$  voltage induced by the 0.001 Hz error of the frequency. (a) The real frequency is 0.3 Hz; (b) The real frequency is 1 Hz

Fig. 6, a relative error of 25 % is induced by 0.001 Hz error of the frequency at 0.3 Hz, while the deviation decreases sharply to a relatively insignificant degree of 2 % as the frequency rises to 1 Hz. This is considered to be the main reason why the commercial lock-in amplifier fails to guarantee its accuracy at frequencies less than 0.4 Hz in this paper.

Then three measurements are carried out at room temperature for commercial polypropylene (PP), commercial polystyrene (PS), and commercial poly (methyl methacrylate) (PMMA), respectively. The  $3\omega$  voltage versus frequency and the corresponding fit of one of the PP samples are plotted in Fig. 7. The symbols are experimental data, and the curve is fit using Eq. 8. It is found that the model fits the data well without considering the interfacial thermal resistance between the wire and the solid samples. The curve fitting results for the thermal conductivity, the thermal diffusivity, and the product of the specific heat and density with their average values and scatters are

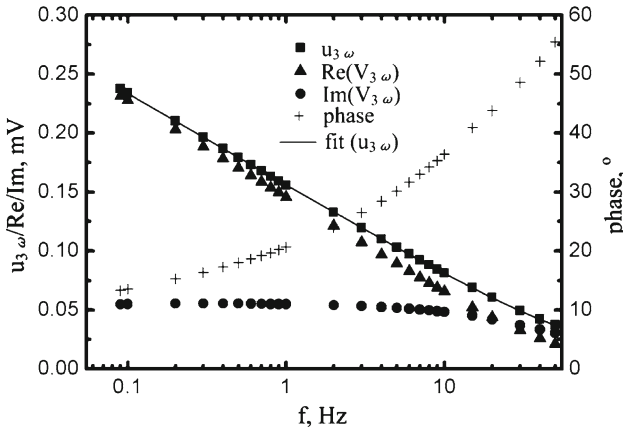


**Fig. 7**  $3\omega$  voltage versus the logarithm of frequency. *Solid squares* indicate the amplitude of the  $3\omega$  voltage, *solid triangles* and *circles* indicate the real and imaginary parts of the  $3\omega$  voltage, *cross symbols* indicate the phase of the  $3\omega$  voltage, and *solid line* is the fit using Eqs. 6 and 8

**Table 1** Measured thermal conductivities,  $\lambda$  ( $\text{W} \cdot \text{m}^{-1} \cdot \text{K}^{-1}$ ) of PP, PS, and PMMA

Polymer	1	2	3	4	$\epsilon^a$	$\Delta^a(\pm\%)$
PP	0.175	0.172	0.176	0.178	0.175	1.85
PS	0.153	0.159	0.154	0.157	0.156	1.92
PMMA	0.204	0.213	0.196	0.201	0.204	4.41

<sup>a</sup>  $\epsilon$ , average value;  $\Delta$ , standard deviation

**Table 2** Measured thermal diffusivities,  $\alpha$  ( $10^{-7} \text{m}^2 \cdot \text{s}^{-1}$ ) of PP, PS, and PMMA

Polymer	1	2	3	4	$\epsilon^a$	$\Delta^a(\pm\%)$
PP	1.85	1.72	1.93	1.63	1.78	8.56
PS	1.49	1.91	1.54	1.88	1.71	12.6
PMMA	2.54	2.33	2.61	2.59	2.52	7.46

<sup>a</sup>  $\epsilon$ , average value;  $\Delta$ , standard deviation

shown in Tables 1, 2, and 3, respectively. It is worth noting that the scatter of the thermal conductivity is much smaller than that of the thermal diffusivity. To evaluate the reliability of the measured thermal properties, the sensitivity,  $s$ , is introduced as

$$s_{\lambda(\alpha)} = \frac{\eta_{u_{3\omega}}}{\eta_{\lambda(\alpha)}} \tag{10}$$

where  $\eta$  is the relative uncertainty, and index  $\lambda, \alpha, u_{3\omega}$ , denote the thermal conductivity, the thermal diffusivity, and the amplitude of the  $3\omega$  voltage, respectively. Figure 8 illustrates the calculated results of the relative uncertainty of the amplitude of the  $3\omega$  voltage perturbed by 1% variation of each thermal property at different frequencies, which indicates that the amplitude of the  $3\omega$  voltage is more sensitive to the thermal



**Table 3** Measured products of specific heat and density,  $\rho c_p$  ( $10^6 \text{ J} \cdot \text{m}^{-3} \cdot \text{K}^{-1}$ ) of PP, PS, and PMMA

Polymer	1	2	3	4	$\epsilon^a$	$\Delta^a(\pm\%)$
PP	0.946	1.00	0.912	1.09	0.987	10.6
PS	1.03	0.832	1.00	0.835	0.924	11.1
PMMA	0.803	0.914	0.751	0.776	0.811	12.7

<sup>a</sup>  $\epsilon$ , average value;  $\Delta$ , standard deviation

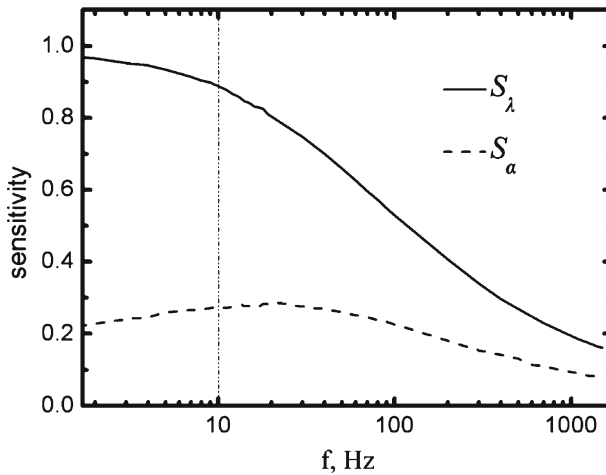


**Fig. 8** Simulation results of Eq. 8: sensitivities of the amplitude of the  $3\omega$  voltage to the thermal conductivity (solid line) and thermal diffusivity (dashed line) as a function of frequency

conductivity than to the thermal diffusivity, especially at low frequencies. In our case, based on the performances of the apparatuses, the frequency range is chosen to cover a relatively low frequency range (0.1 Hz to 10 Hz) to ensure that the  $3\omega$  voltage has sufficient resolution. It is the main reason why the measured thermal conductivities have better reproducibility here. However, more reliable thermal-diffusivity results can be obtained if a higher precision of the measurement could be attained and frequencies for the measurement are chosen to cover a higher frequency range from 1 Hz to 50 Hz. Table 4 shows the average values (Column A) of the thermal conductivities obtained for PP, PS, and PMMA, which are in good agreement with corresponding values found in the literature (Column B) [7].

A careful analysis of the uncertainty of the results is also very crucial when a technique is newly proposed. Errors of the method can be evaluated by considering three possible sources of errors: errors introduced by the measurement procedure, errors caused by the deviations of the actual experimental condition from the theoretical model, and errors due to the non-linear regression analysis procedure. Considering the first source of errors, the uncertainty of the thermal conductivity can be given by the error transfer function [8]. Here, it is assumed that the thermal diffusivity of the sample is known as a constant. The diameter of the hot wire is measured by a scanning electron microscope (SEM), causing an uncertainty of the thermal conductivity of 1%.

**Table 4** Thermal conductivities,  $\lambda$  ( $\text{W} \cdot \text{m}^{-1} \cdot \text{K}^{-1}$ ) of PP, PS, and PMMA

Polymer	Column A	Column B [7]
PP	$0.175 \pm 0.0053$	0.172
PS	$0.156 \pm 0.0047$	0.142
PMMA	$0.204 \pm 0.0061$	0.193

The uncertainty of the dc resistance of the hot wire and the  $3\omega$  voltage signal are both within 0.1 %. The length of the hot wire is obtained from its diameter and resistance, causing an estimated uncertainty of 2 %. The uncertainty caused by the amplitude of the current is too small to be neglected. As a result, the overall uncertainty of the measured thermal conductivities introduced by the measurement procedure is evaluated, which lies within 3 %. The second source of errors is associated with the deviations of the actual experimental condition from the assumptions of the theoretical model, such as  $l_h \gg r_h$ , axis symmetry, uniform temperature along the hot-wire radius, and infinite sample size. The appropriate choice of dimensions of the hot wire and tested samples as well as the frequency range for the measurement is critical to minimize the second source of errors. In addition, the contact condition between the samples and the hot wire is also responsible for the second source of errors. In the non-linear regression analysis process, the accuracy of the fit can be evaluated by calculating the correlation coefficient, which is given by

$$R = \frac{\sum_{i=1}^N y_i(\text{mea})y_i(\text{fit}) - \frac{1}{N} \sum_{i=1}^N y_i(\text{mea}) \sum_{i=1}^N y_i(\text{fit})}{\left\{ \left[ \sum_{i=1}^N y_i(\text{mea})^2 - \frac{1}{N} \left( \sum_{i=1}^N y_i(\text{mea}) \right)^2 \right] \times \left[ \sum_{i=1}^N y_i(\text{fit})^2 - \frac{1}{N} \left( \sum_{i=1}^N y_i(\text{fit}) \right)^2 \right] \right\}^{1/2}} \quad (11)$$

where  $y_i(\text{mea})$  and  $y_i(\text{fit})$  are measured results and fitted results, respectively, and  $N$  is the total number of experimental points. All the correlation coefficients in this work lie around 0.999, which lead to negligible error when compared with other sources of errors. Therefore, the overall uncertainty in the calculation of the thermal conductivity of the polymers using the system in this study is estimated to be around 3 %.

The virtual  $3\omega$  measurement technique inherits both the advantage of the hot-wire technique [8] that the sample is easily prepared and the advantage of the traditional  $3\omega$  technique that the two thermal properties (thermal conductivity and thermal diffusivity) can be simultaneously determined. Furthermore, it has three specific advantages when compared with them: (a) In this method, samples are prepared in the shape of 3 mm thick rectangles and the mass of the material involved in the paper is approximately 100 mg, which is much smaller than the size of samples applied in the case of the steady-state hot-wire technique [8]. This fact can considerably reduce the time interval required for the sample to reach thermal equilibrium at different measurement temperatures. Besides, the present method uses a short hot wire about 10 mm long as the probe, which solves the problem of inhomogeneity in polymer samples; (b) compared to traditional  $3\omega$  systems employing commercial lock-in amplifiers, the LabVIEW-based virtual lock-in amplifier has higher accuracy for low frequency measurements, brings flexibility and scalability to the measurement system, and largely

reduces the cost of the experimental setup; (c) based on the high scalability of the technique, the measurement system can be easily developed to meet other measurement requirements such as measuring polymers at different temperatures and states.

## 5 Conclusions

- (1) It is easy and convenient to prepare samples by pressing the Pt hot wire into the interface of the two-folded polymers in the molten state.
- (2) The computer-based virtual digital lock-in-amplifier has proved to work well as a substitute for the commercial instrument, with such advantages as good performance at low frequency, high flexibility/scalability, and low cost.
- (3) The  $3\omega$  measurement technique is an effective way to determine the thermal conductivity of polymers with good accuracy and reproducibility. The uncertainty of the measurement is estimated to be 3 % for thermal conductivity.

**Acknowledgments** This study was supported by the National Natural Science Foundation of China (Grant Nos. 50676046 and 50730006).

## References

1. M. Luba, T. Pelt, G.R. Griskey, *J. Appl. Polym. Sci.* **23**, 55 (1979)
2. G.M. Kulkarni, A.R. Mashelkar, *Polymer* **22**, 867 (1981)
3. G.D. Cahill, O.R. Pohl, *Phys. Rev. B* **35**, 4067 (1987)
4. F. Chen, J. Shulman, Y.Y. Xue, W.C. Chu, *Rev. Sci. Instrum.* **75**, 11 (2004)
5. Z.L. Wang, D.W. Tang, X.H. Zhen, W.F. Bu, W.G. Zhang, *J. Eng. Thermophys.* **28**, 3 (2007)
6. L. Lu, W. Yi, L.D. Zhang, *Rev. Sci. Instrum.* **72**, 7 (2001)
7. W.D. Van Krevelen, J.P. Hoftyzer, *Properties of Polymers, Their Estimation and Correlation with Chemical Structure*, 2nd edn. (Elsevier, Scientific Publishing Company, Amsterdam, Oxford, New York, 1976), p. 400, Table 17.1
8. Wilson Nunes dos Santos, *Polym. Test.* **24**, 932 (2005)